

## Investigation of low-lying magnetic dipole excitations in the $^{153}\text{Eu}$ nucleus

Emre TABAR<sup>1,2,\*</sup>

<sup>1</sup>Department of Physics, Faculty of Science and Arts, Sakarya University, Sakarya, Turkey

<sup>2</sup>Biomedical, Magnetic and Semiconductor Materials Research Center (BİMAYAM), Sakarya University, Sakarya, Turkey

Received: 14.10.2016

Accepted/Published Online: 20.12.2016

Final Version: 18.04.2017

**Abstract:** The properties of low-lying magnetic dipole ( $M1$ ) excitations in  $^{153}\text{Eu}$  were studied within a rotational invariant quasiparticle phonon model that takes into account the symmetry-restoring as well as spin–spin residual forces. The calculations show that there are purely collective  $M1$  excitations lying at 2–4 MeV fragmented over orbital  $1^+$  states of the  $^{152}\text{Sm}$  core nucleus. The results were compared to the experimentally known  $M1$  excitations at 2–3 MeV. A reasonably good agreement in the total transition strength, the centroid energy, and the resonance width was obtained.

**Key words:**  $^{153}\text{Eu}$ ,  $M1$  excitations, scissors mode, rotational invariance, quasiparticle phonon model

### 1. Introduction

The low-lying magnetic dipole ( $M1$ ) strength in atomic nuclei is almost completely constituted by the scissors mode. From a geometrical point of view, scissors mode is described as an oscillation of the deformed neutron system against the deformed proton system [1]. The scissors mode has been investigated intensively by both experimentalists and theoreticians since the first experimental discovery of it in  $^{156}\text{Gd}$  in 1984 [2]. These extensive studies have provided us a large body of information on the systematics of this mode particularly in even–even nuclei over a wide mass range from light to actinide region (for a review see [1,3]).

The mode in odd-mass nuclei was first observed in  $^{163}\text{Dy}$  (in 1993) where the observed dipole strength was fit into the systematics of the scissors mode in the neighboring even–even  $^{164,162,160}\text{Dy}$  isotopes [4]. After this discovery, a large number of both experimental and theoretical works were stimulated [1, and the references therein]. From the theoretical point of view, the scissors mode in odd-mass nuclei has been analyzed with several models. Some examples are the interacting boson fermion model (IBFM), generalized coherent-state model, sum rule approaches, and group theory approaches [1,3]. However, these models do not reproduce the fragmentation of the  $M1$  strength, which is of crucial importance in odd-mass nuclei. The fragmentation of  $M1$  strength in odd-mass nuclei can be explained using microscopic models such as quasiparticle random phase approximation (QRPA) or the more general quasiparticle phonon nuclear model (QPNM). However, in these models the rotational symmetry of the single particle Hamiltonian simultaneously is violated by the Hartree–Fock–Bogoliubov (HFB) approaches in the mean field [5–7]. The violation of the rotational invariance results in admixtures (spurious states) connected with rotational degree of freedom in  $K^\pi = 1^+$  excitation states of even–even core [7,8]. One has to remove these spurious contributions to determine exactly the energies of excitation

\*Correspondence: etabar@sakarya.edu.tr

states and the  $M1$  strength distribution in odd-mass nuclei. It has been recently shown that for odd mass nuclei it is possible to obtain the precise restoration of the rotational symmetry of the QPNM Hamiltonian in the framework of the separable isoscalar and isovector residual interaction [9,10]. The method originally proposed by Kuliev et al. for the elimination of the spurious states in deformed even–even nuclei [7] successfully described the low-lying magnetic dipole excitations in even–even rare-earth [11], gamma-soft [12], and actinide nuclei [13].

In the present paper, the low-lying  $M1$  transitions, so-called scissors mode, are theoretically investigated in deformed odd-mass  $^{153}\text{Eu}$  nucleus in the framework of the rotational invariant (RI-) QPNM for the first time. The study of the scissors mode in the  $^{153}\text{Eu}$  nucleus deserves special attention since the dipole strength distributions in its core  $^{152}\text{Sm}$  were investigated by both experimentalists [14] and theorists [7].

## 2. Theory

The general form of the QPM Hamiltonian is

$$H \approx H_{sqp} + H_{coll.} + H_{int.}, \quad (1)$$

where

$$H_{sqp} = \sum_{s,\tau} \varepsilon_s \alpha_{s\rho}^+ \alpha_{s\rho} \quad (2)$$

$$H_{coll.} = \frac{1}{2} \sum_{\tau\tau'} \chi_{\tau\tau'} \sum_{ss'} \sigma_{ss'}^{(\mu)} L_{ss'} g_{ss'}^i [Q_{i\mu}^+(\tau) + Q_{i\mu}(\tau)] \times \sum_{tt'} \sigma_{tt'}^{(\mu)} L_{tt'} g_{tt'}^i [Q_{i\mu}^+(\tau') + Q_{i\mu}(\tau')] \quad (3)$$

$$H_{int.} = \frac{1}{2} \sum_{\tau\tau'} \chi_{\tau\tau'} \sum_{tt'} \sum_{ss'} \left\{ \sigma_{ss'}^{(\mu)} M_{ss'} \sigma_{tt'}^{(\mu)} L_{tt'} g_{tt'}^i D_{ss'} [Q_{i\mu}^+(\tau') + Q_{i\mu}(\tau')] + \sigma_{ss'}^{(\mu)} L_{ss'}^T \sigma_{tt'}^{(\mu)} M_{tt'} g_{ss'}^i [Q_{i\mu}^+(\tau) + Q_{i\mu}(\tau)] D_{tt'} \right\} \quad (4)$$

Here  $H_{sqp}$  describes the motion of quasiparticles and includes pairing correlations,  $H_{coll.}$  represents the collective motion of nucleons, and  $H_{int.}$  describes connection [9,10].

In Eqs. (3) and (4), ;  $g_{ss'}^i(\tau) = \psi_{ss'}^i(\tau) + \phi_{ss'}^i(\tau)$ ,  $ss'(tt')$  represents the single-particle states of the axially symmetric Woods–Saxon potential for neutrons (protons).  $M_{ss'} = u_s u_{s'} + v_s v_{s'}$  and  $L_{ss'} = u_s v_{s'} - u_{s'} v_s$ , where  $u_s$  and  $v_s$  are the Bogoliubov transformation coefficients and  $\varepsilon_s(\tau)$  are the energies of one-quasiparticle states.  $\alpha_{s\rho}^+(\tau)$  and  $Q_{i\mu}^+$  are creation operators of quasiparticles and phonons, respectively. The quantities  $\sigma_{ss'}^{(\mu)} = \langle s | \sigma_\mu | \rangle$  and  $D_{ss'}^T$  are the matrix elements of the Pauli spin operator and the two-quasiparticle operators, respectively. The coupling constants of spin–spin residual force are  $\chi_{nn} = \chi_{pp} = \chi$  and  $\chi_{np} = q\chi$  for the neutron–neutron, proton–proton, and neutron–proton interactions. The coupling constant can be described in terms of interaction strength ( $\kappa$ ), i.e.  $\chi = \frac{\kappa}{A}$  MeV [9,10].

The wave function for an odd-mass nucleus describing the nonrotational states with a fixed value of  $K^\pi$  can be written as follows:

$$\psi_K^j(\tau) = \left\{ \sum_q N_{s_q}^j(\tau) \alpha_{s_q}^+(\tau) + \sum_{i\mu} \sum_\nu G_j^{i\mu\nu} \alpha_\nu^+(\tau) Q_{i\mu}^+ \right\} |\psi_0\rangle \quad \mu = 0, \pm 1 \quad (5)$$

with the normalization condition

$$\langle \psi_K^j(\tau) | \psi_K^j(\tau) \rangle = \sum_q \left( N_{\varsigma_q}^j \right)^2 + \sum_{i\mu} \sum_{\nu} \left( G_j^{i\mu\nu} \right)^2 = 1, \quad (6)$$

where  $\psi_0$  is the wave function of the ground-state of even-even core, i.e. phonon vacuum. The integer  $j = 1, 2, 3, \dots$  is the number of the state, and  $\varsigma$  and  $\nu$  denote the quantum numbers of a one-quasiparticle state. The quantities  $N_{\varsigma_q}^j$  and  $G_j^{i\mu\nu}$  define the contribution of the one-quasiparticle and quasiparticle  $\otimes$  phonon component to the normalization condition [9,10].

Because of the axially symmetric isoscalar and isovector terms of the mean field potential, the rotational invariance of  $H_{sqp}$  is simultaneously broken. The broken rotational symmetry can be restored by including the effective isoscalar ( $h_0$ ) and isovector ( $h_1$ ) forces in the following form:

$$h_0 = -\frac{1}{2\gamma_0} \sum_{\mu=\pm} [H_{sqp} - V_1, J_\mu]^+ [H_{sqp} - V_1, J_\mu] \quad (7)$$

$$h_1 = -\frac{1}{2\gamma_1} \sum_{\mu=\pm} [V_1, J_\mu]^+ [V_1, J_\mu] \quad (8)$$

In Eqs. (7) and (8),  $J_\mu$  total angular momentum operator can be written as the summation of two terms  $J_\mu = J_\mu^{qp} + J_\mu^{bos.}$ , where in the quasiparticle-phonon representation

$$J_\mu^{qp} = \sum_{ss'} j_{ss'}^{(\mu)} M_{ss'} D_{ss'} \quad (9)$$

$$J_\mu^{bos.} = \sum_{ss'} j_{ss'}^{(\mu)} L_{ss'} (Q_{i\mu}^+ + Q_{i\mu}) \quad (10)$$

If Eqs. (9) and (10) are written in Eqs. (7) and (8), one can see that Eqs. (7) and (8) separate into quasiparticle ( $qp$ ), boson ( $bos.$ ), and interaction ( $int.$ ) terms. The quasiparticle term causes a small energy shift of one-quasiparticle spectra and does not affect the  $M1$  distributions. Therefore, only boson and interaction terms are taken into account in the calculation of  $M1$  strength in odd-mass nuclei. Therefore, the violated rotational symmetry of QPNM Hamiltonian of odd-mass nuclei can be restored using the separable residual interaction in the following form [9,10]:

$$\begin{aligned} h_0^{bos.} &= \frac{-1}{2\gamma_0} \sum_{\mu=\pm 1} [H_{sqp} - V_1, J_\mu^{bos.}]^+ [H_{sqp} - V_1, J_\mu^{bos.}] \\ h_0^{int.} &= \frac{-1}{2\gamma_0} \sum_{\mu=\pm 1} \left\{ [H_{sqp} - V_1, J_\mu^{qp}]^+ [H_{sqp} - V_1, J_\mu^{bos.}] + h.c. \right\} \end{aligned} \quad (11)$$

$$\begin{aligned} h_1^{bos.} &= \frac{-1}{2\gamma_1} \sum_{\mu=\pm 1} [V_1, J_\mu^{bos.}]^+ [V_1, J_\mu^{bos.}] \\ h_1^{int.} &= \frac{-1}{2\gamma_1} \sum_{\mu=\pm 1} \left\{ [V_1, J_\mu^{qp}]^+ [V_1, J_\mu^{bos.}] + h.c. \right\} \end{aligned} \quad (12)$$

Here  $V_1$  is the isovector potential [7] and  $J_\mu$  ( $\mu = \pm 1$ ) is angular momentum operator. *h.c.* means hermitic conjugate. In Eqs. (11) and (12) the coupling constants  $\gamma_0$  and  $\gamma_1$  are determined self-consistently by the mean-field parameters [9,10]

$$\begin{aligned}\gamma^{(\mu=\pm)} &= \langle \psi_{K_0} | [J_\mu^+, [H_{sqp}, J_\mu]] | \psi_{K_0} \rangle \\ \gamma_1^{(\mu=\pm)} &= \langle \psi_{K_0} | [J_\mu^+, [V_1, J_\mu]] | \psi_{K_0} \rangle\end{aligned}\quad (13)$$

where

$$\begin{aligned}\gamma^{(-1)} = \gamma^{(+1)} = \gamma & \quad ; \quad \gamma_1^{(-1)} = \gamma_1^{(+1)} = \gamma_1 \\ \gamma_0 = \gamma - \gamma_1 & \quad ; \quad \gamma = \gamma^n + \gamma^p & \quad ; \quad \gamma_1 = \gamma_1^n - \gamma_1^p\end{aligned}\quad (14)$$

In Eq. (9)  $|\psi_{K_0}\rangle = \alpha_{s_0}^+ |\psi_0\rangle$  is the ground-state wave function of an odd-mass nucleus, where  $\psi_0$  corresponds to a phonon vacuum. The energies of the nonrotational states in odd-mass nuclei are determined by means of the variational principle, i.e.

$$\delta \left\{ \langle \psi_K^j(\tau) | H_{inv.} | \psi_K^j(\tau) \rangle - \langle \psi_K^j(\tau) | H_{inv.} | \psi_{K_0}(\tau) \rangle - \eta_K^j \left[ \sum_q \left( N_{s_q}^j \right)^2 + \sum_{i\mu} \sum_\nu \left( G_j^{i\mu\nu} \right)^2 - 1 \right] \right\} = 0 \quad (15)$$

After performing a variational procedure and some transformations, we obtain the following secular determinant [9,10]:

$$\det \begin{pmatrix} (\varepsilon_{s_1} - \eta_K) - F_\tau(s_1, s_1) & -F_\tau(s_1, s_2) & \dots & -F_\tau(s_1, s_m) \\ -F_\tau(s_2, s_1) & (\varepsilon_{s_2} - \eta_K) - F_\tau(s_2, s_2) & \dots & -F_\tau(s_2, s_m) \\ \dots & \dots & \dots & \dots \\ -F_\tau(s_m, s_1) & -F_\tau(s_m, s_2) & \dots & (\varepsilon_{s_m} - \eta_K) - F_\tau(s_m, s_m) \end{pmatrix} = 0 \quad (16)$$

where

$$H_{inv.} = H_{sqp} + H_{coll.} + H_{int.} + h_0^{boz.} + h_0^{int.} + h_1^{boz.} + h_1^{int.} \quad (17)$$

$$F_\tau(s_q, s_m) = \sum_{i\nu} \frac{\Lambda_{i\nu}(s_q, \tau) \Lambda_{i\nu}(s_m, \tau)}{(\omega_i + \varepsilon_\nu - \eta_K^j)} \quad \Lambda_{i\nu}(s_q, \tau) = \chi R_Q^i(\tau, \tau') M_{s_q\nu} \sigma_{s_q\nu}^{(J)}(i) \quad (18)$$

$$\sigma_{s_q\nu}^{(J)}(i) = \sum_\mu \left\{ \sigma_{s_q\nu}^{(\mu)} - j_{s_q\nu}^{(\mu)} \left[ \frac{\gamma_1 R_0^i(\tau) \varepsilon_0^{(-)} - (\gamma - \gamma_1) R_1^i(\tau) V_1^{(-)}}{\chi R_Q^i(\tau, \tau') (\gamma - \gamma_1) \gamma_1} \right] \right\} \quad (19)$$

Here

$$\begin{aligned}R_0^i(\tau) &= \sum_{ss'} \varepsilon_{ss'}^0 j_{ss'}^{(\mu)} L_{ss'} w_{ss'}^i & ; & \quad \varepsilon_{ss'}^0 = (\varepsilon_{ss'}^\tau - \tau_z V_{1ss'}^\tau) & ; & \quad V_{1\tau}^{(-)} = V_{1s_q}^\tau - V_{1\nu}^\tau \\ R_1^i(\tau) &= \sum_{ss'} V_{1ss'} j_{ss'}^{(\mu)} L_{ss'} w_{ss'}^i & ; & \quad w_{ss'}^i = \psi_{ss'}^i(\tau) - \phi_{ss'}^i(\tau) & ; & \quad \varepsilon_0^{(-)} = \varepsilon_\tau^{(-)} - \tau_z V_\tau^{(-)}\end{aligned}\quad (20)$$

$$R_Q^i(\tau, \tau') = R_\tau^i + q R_{\tau'}^i = \begin{cases} R_n^i + q R_p^i, & \text{odd} - N \\ R_p^i + q R_n^i, & \text{odd} - P \end{cases} ; \quad R_{\tau'}^i = \sum_{ss'} \sigma_{ss'} L_{ss'} g_{ss'}^i \quad (21)$$

In Eq. (18),  $\omega_i$  denotes the energy of the collective vibrational state of even–even core. Here  $\eta_K^j$  ( $j = 1, 2, 3, \dots$ ) are the roots of the secular equation from which the energies of the nonrotational states in odd-mass nuclei are determined.  $q$  is the number of the average field levels with a given  $K^\pi$ . Using the normalization condition and the secular equation, analytical formulae for the functions  $G_j^{i\mu\nu}$  and  $N_{\zeta_q}^j$  amplitudes of the wave function can be derived [9,10].

The formula for the reduced probabilities of  $M1$  transitions from the ground states to the excited states of odd-mass nuclei can be written in the form

$$B(M1 \uparrow; I_0 K_0 \rightarrow IK) = \langle I_0 K_0 1\mu | IK \rangle^2 \left| -N_{\zeta_0} \sum_q N_{\zeta_q}^j m_{\zeta_q \zeta_0}^{(\mu)}(\tau) M_{\zeta_q \zeta_0} + N_{\zeta_0} \sum_{\tau} \sum_{j,i\mu} \sum_{ss'} m_{ss'}^{(\mu)}(\tau) L_{ss'} g_{ss'}^i G_{j i \mu}^{v \zeta_0} \right|^2 \quad (22)$$

where  $m_{ss'}^{(\mu)}(\tau) = \sqrt{\frac{3}{4\pi}} [(g_s^\tau - g_l^\tau) \langle s | s_\mu^\tau | \rangle + g_l^\tau \langle s | J_\mu^\tau | \rangle]$   $\mu_N$  are the single particle matrix elements of the  $M1$  operator [9, 10].  $E1$  and  $M1$  transitions in odd-mass nuclei have not been experimentally distinguished. Therefore, the magnetic dipole radiation widths have been calculated using

$$g\Gamma_0(M1) = 11.547 \times E_\gamma^3 \times B(M1 \uparrow) \quad [meV] \quad (23)$$

$$g\Gamma_0^{red}(M1) = 11.547 \times B(M1 \uparrow) \quad [meV MeV^{-3}] \quad (24)$$

relations, where  $g = \frac{2J_0+1}{2J+1}$  [9,10].

### 3. Results and discussion

The calculations were performed with the single-particle energies and wave functions of an axially symmetric Woods–Saxon potential [15] with  $\beta_2 = 0.3064$  (27) quadrupole deformation parameter derived from the experimental quadrupole moment [16]. The single-particle spectrum was taken from the bottom of the potential well up to +5 MeV. The proton and neutron pairing interaction constants,  $\Delta_p = 0.806$  and  $\Delta_n = 0.949$ , were chosen based on the single-particle levels. The strength of the spin–spin interaction ( $\kappa = 45$  MeV) was determined by comparison of the theoretical and the experimental values of ground-state intrinsic magnetic moments ( $g_K$ ). In order to compute the  $M1$  strengths, the effective gyromagnetic factor ( $g_s^{eff} = 0.55g_s^\tau$ ) derived by the ground-state calculation of the  $^{153}\text{Eu}$  nucleus was used. The normalization of the  $g_s^\tau$  factor was due to the spin polarization of the doubly even core.

The ground-state spin and parity of  $^{153}\text{Eu}$  was experimentally found to be  $I_0^\pi = 5/2^+$  [17]. Therefore, the states with  $I_f^\pi = 3/2^+$  and  $I_f^\pi = 7/2^+$  can be excited by magnetic dipole transitions. Accordingly, the reduced transition probabilities, i.e.  $B(M1)$  values from the ground-state ( $I_0 K_0$ ) to all excited states in  $^{153}\text{Eu}$  with  $I_f K_f$  were calculated in RI-QPNM. In the calculations phonon basis was constructed by  $I^\pi K = 1^+ 1$  RI-QRPA phonons of doubly even core. In order to obtain a good description of the low-lying  $M1$  spectra in odd-mass nuclei, the  $M1$  strength distributions in the corresponding even–even core should be studied accurately. The success of the RI-QRPA in the description of the low-lying  $M1$  distribution in  $^{152}\text{Sm}$  used to construct the phonon basis of  $^{153}\text{Eu}$  is demonstrated in Table 1 by the comparison of RI-QRPA results with two-rotor model (TRM) [18] and projected Hartree–Fock–Bogoliubov (PHFB) [19] calculations, and with the experimental data [20].

**Table 1.** Comparison of RI-QRPA results for summed  $M1$  strength and energy centroid of  $M1$  resonance in  $^{152}\text{Sm}$  with experimental data [12] and with other theoretical studies.

	Theory				Experiment [14]
	RI-QRPA		TRM	PHFB	
	2–3 MeV	2–4 MeV	2–4 MeV	2–4 MeV	2–4 MeV
$\sum_{I_f} B(M1 \uparrow) [\mu_N^2]$	1.25	2.37	2.35	2.53	$2.35 \pm 0.11$
$\bar{E}$ [MeV]	2.91	3.24	3.05	3.29	2.98

Figure 1 shows the theoretical and experimental  $M1$  strength distribution for  $^{153}\text{Eu}$ . In the lower and upper parts of Figure 1 the experimental data are compared to RI-QPNM and nonrotational invariant (NRI-) QPNM results, respectively.

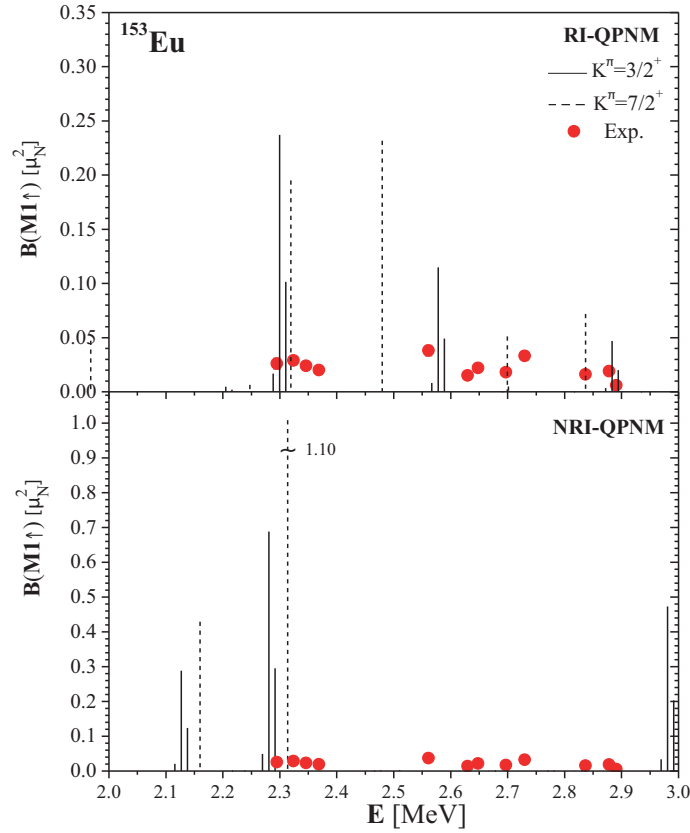


**Figure 1.**  $M1$  spectrum obtained from RI-QPNM and NRI-QPNM calculations compared to experiment [18].

As seen from Figure 1, because of the coupling properties of the  $M1$  operator, the states with  $K_f = K_0 - 1$  are more fragmented than the states with  $K_f = K_0 + 1$ . The distribution of the experimental  $B(M1)$  values can satisfactorily be described within the RI-QPNM taking into account isoscalar and isovector symmetry restoring interactions simultaneously. The inclusion of the symmetry restoring interactions leads, in comparison with the results of NRI-QPNM, to a more than two order of magnitude decrease in the calculated  $B(M1)$  values. The summed QPNM strength in the energy range 2–3 MeV is  $\sum_{I_f} B(M1 \uparrow) = 1.168 \mu_N^2$  whereas the

summed NRI-QPNM strength in this interval is  $\sum_{I_f} B(M1 \uparrow) = 3.90 \mu_N^2$ . This case is due to the elimination of spurious states arising from broken rotational symmetry of the single quasiparticle Hamiltonian in RI-QPNM. In addition, the calculated  $M1$  strength in RI-QPNM is more fragmented in comparison with the NRI-QPNM results. The orbital-spin ratios ( $l/s$ ) ranging from 2.1 to 34.7 for RI-QPNM  $M1$  states indicate that the low-energy  $M1$  states (2–4 MeV) are exclusively orbital excitations. This result is in agreement with the conclusion [1,3] about the orbital character of the low-lying  $M1$  excitations, so-called scissors mode, in deformed doubly even-mass nuclei.

For a more quantitative evaluation of theoretical results, the predictions of RI-QPNM for gross features of  $M1$  transitions in  $^{153}\text{Eu}$  are compared in Table 2 with experimental data [20].

**Table 2.** Comparison of the predictions of RI-QPNM for gross features of  $M1$  transitions in  $^{153}\text{Eu}$  with experimental data [12].

$K^\pi$	Theory				Experiment [20]			
	$\sum_{I_f} B(M1 \uparrow)$ [ $\mu_N^2$ ]	$\sum_{I_f} \Gamma_0(M1)$ [meV]	$\sum_{I_f} \Gamma_0^{red}(M1)$ [meV MeV $^{-3}$ ]	$\bar{E}$ [MeV]	$\sum B(M1 \uparrow)$ [ $\mu_N^2$ ]	$\sum \Gamma_0(M1)$ [meV]	$\sum \Gamma_0^{red}(M1)$ [meV MeV $^{-3}$ ]	$\bar{E}$ [MeV]
$3/2^+$	0.606	106.25	7.009	2.457	-	-	-	-
$7/2^+$	0.562	98.30	6.504	2.457	-	-	-	-
All	1.168	204.55	13.513	2.456	$0.338 \pm 0.06$	$54.08 \pm 8.5$	$3.91 \pm 0.64$	2.263

The experimental centroid energy of 2.263 MeV is quite well reproduced by RI-QPNM ( $\bar{E} = 2.456 \text{ MeV}$ ) while the summed transition strength calculated in RI-QPNM is almost 3 times larger than the experimental one. On the other hand, as seen from Table 1, the summed  $M1$  strength predicted by RI-QPNM in odd-mass  $^{153}\text{Eu}$  in 2–3 MeV energy interval should be nearly equal to that calculated using RI-QRPA for the core nucleus, i.e.  $^{152}\text{Sm}$ . However, the degree of fragmentation increased going from even–even mass  $^{152}\text{Sm}$  to odd-mass  $^{153}\text{Eu}$ .

The transition strength in odd-mass nuclei becomes highly fragmented owing to the high level densities. Therefore, a large part of the strength remains unresolved in the background of the NRF spectra of the deformed odd-mass nuclei. With the available experimental techniques the detection of these weak transition strengths is impossible [20,21]. It was shown that the missing strength can be extracted from the background by means of a statistical fluctuation analysis method [22]. However, this method has not been applied to the proton-odd nucleus  $^{153}\text{Eu}$  so far. Fluctuation analysis for  $^{153}\text{Eu}$  would give us a better opportunity to compare the QPNM results.

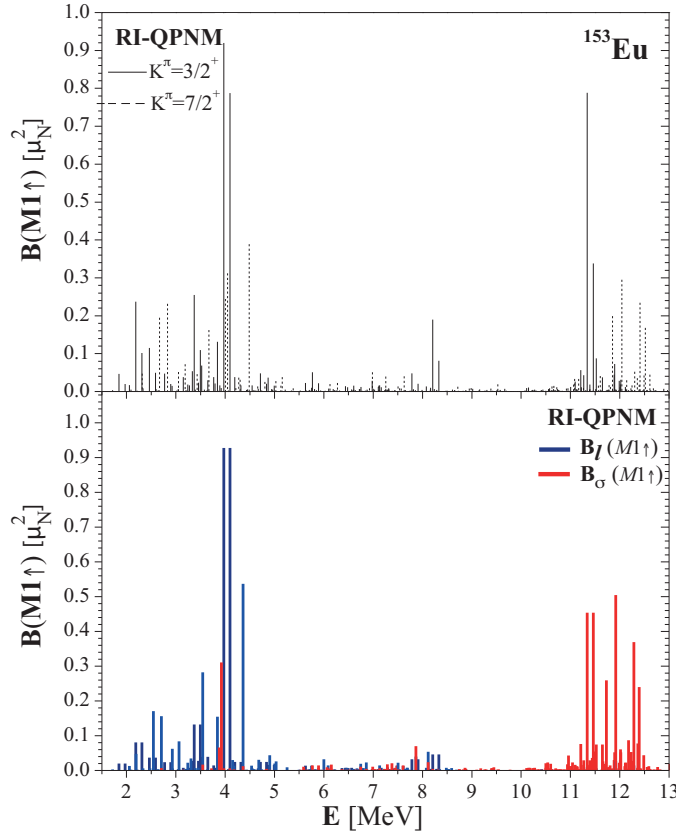
It is of special interest to discuss in more detail the sources of  $M1$  transition strength predicted by the RI-QPM. Therefore, the microscopic structure of low-lying  $M1$  states with  $\sum_{I_f} B(M1 \uparrow) \geq 0.1 \mu_N^2$  in  $^{153}\text{Eu}$  is presented in Table 3. Here, one-quasiparticle components as well as the quasiparticle  $\otimes$  one-phonon ones whose contribution to the normalization condition of the wave function is more than 1% are shown. It should be emphasized that in states above 1.5 MeV the quasiparticle  $\otimes$  one-phonon components are dominant. As seen from Table 3, the contributions of the one-quasiparticle components to normalization of wave function are smaller than 1%. As a result, the dominant component in the region of 2–3 MeV is  $[413] \downarrow \otimes Q_i$ . This indicates that the low-lying  $M1$  states (2–3 MeV) in odd-mass  $^{153}\text{Eu}$  are collective.

**Table 3.** The structure of low-lying  $M1$  states with  $\sum_{I_f} B(M1 \uparrow) \geq 0.1 \mu_N^2$  in  $^{153}\text{Eu}$  in 2–3 MeV.

$E[\text{MeV}]$	$\sum_{I_f} B(M1 \uparrow)[\mu_N^2]$	$K^\pi$	$N_{K\zeta q}^j$	$G_{ij}^{K\zeta q v}$	Structure
2.286	0.195	$7/2^+$	0.054	0.998	99.63% $[413] \downarrow \otimes Q_3$
2.310	0.237	$3/2^+$	0.052	0.999	99.48% $[413] \downarrow \otimes Q_3 + 8.05\% [413] \downarrow \otimes Q_4$
2.315	0.102	$3/2^+$	0.052	0.999	99.48% $[413] \downarrow \otimes Q_3 + 8.05\% [413] \downarrow \otimes Q_4$
2.446	0.232	$7/2^+$	0.060	0.998	99.53% $[413] \downarrow \otimes Q_4$
2.588	0.115	$3/2^+$	0.140	0.990	2.96% $[413] \downarrow \otimes Q_3 + 59.34\% [413] \downarrow \otimes Q_4 + 8.86\% [413] \downarrow \otimes Q_5 + 15.11\% [413] \downarrow \otimes Q_6 + 7.96\% [413] \downarrow \otimes Q_7 + 1.03\% [413] \downarrow \otimes Q_{17}$

From the systematic analyses of  $M1$  strength distribution in deformed even-mass nuclei it is well known that two different classes of magnetic excitations exist [1]. The states from 2 MeV up to about 4 MeV have large orbital contributions, whereas the higher excitations are predominantly of the spin-flip type. Our interest is now in orbital and spin  $M1$  strength distributions in odd-mass  $^{153}\text{Eu}$ . The result of the QPNM calculation of the total, orbital, and spin  $M1$  strengths in the energy range 1.5–13 MeV is presented in Figure 2.

Figure 2 shows that spin–spin interactions shift the spin strength from low to higher energies and increase the orbital character of the low-lying  $M1$  excitations and spin  $M1$  states between 10 and 13 MeV. As also seen from Figure 2, spin  $M1$  strength is highly fragmented. The summed transition strength is


**Figure 2.** The  $M1$  spectrum of the obtained RI-QPNM solutions for  $^{153}\text{Eu}$  together with orbital and spin  $M1$  strengths in 1.5–13 MeV.



$\sum_{I_f} B(M1 \uparrow) = 3.389 \mu_N^2$  in 10–13 MeV. The centroid of this spin resonance is located at 11.8 MeV. There has been no experimental indication of the corresponding spin  $M1$  strength in deformed odd-mass nuclei yet. However, it is well known that there are spin-flip resonances in even–even deformed nuclei above 7–8 MeV. Here the first theoretical predictions for spin  $M1$  excitations in the odd-mass  $^{153}\text{Eu}$  nucleus are given and it may be of interest for experimentalists.

#### 4. Conclusion

Within a microscopic approach (RI-QPNM) that includes effective restoration forces as well as spin–spin residual interaction low-lying  $M1$  excitations were investigated in the well-deformed  $^{153}\text{Eu}$  nucleus. In order to judge the quality of RI-QPNM's predictions the results of another theoretical approach (NRI-QPNM) and the comparisons of these two approaches with the experimental data were also given. For RI-QPNM, good agreement with experiment results in the centroid energy and the distribution of  $M1$  strength was obtained. However, RI-QPNM results for transition strength and width were three times higher than those observed in the experiment. This discrepancy is due to the hidden strength in background of the NRF spectra and so fluctuation analysis is needed for an exact comparison of RI-QPNM results for  $^{153}\text{Eu}$ .

RI-QPNM calculations predict strong and pure spin  $M1$  excitations around 10–13 MeV. In this context, an experimental search for high-lying  $M1$  strengths would be very interesting.

On the basis of this investigation, it is possible to conclude that introduction of effective restoration forces in QPNM is sufficient to explain the experimentally observed fragmentation in  $M1$  spectra of  $^{153}\text{Eu}$ .

#### Acknowledgments

I express my gratitude to Dr H Yakut and Prof AA Kuliev for their valuable contributions and stimulating discussions. The financial support from the Scientific and Technological Research Council of Turkey (TÜBİTAK) (Project no. 115F564) is gratefully acknowledged.

#### References

- [1] Heyde, K.; Von Neumann-Cosel, P.; Richter, A. *Rev. Mod. Phys.* **2010**, *82*, 2365-2419.
- [2] Bohle, D.; Richter, A.; Steffen, W.; Dieperink, A.; Lo Iudice, N.; Palumbo, F.; Scholten, O. *Phys. Lett. B* **1984**, *137*, 27-31.
- [3] Lo Iudice, N. *Phys. Part. Nucl.* **1997**, *28*, 556-585.
- [4] Bauske, I.; Arias, M.; Von Brentano, P.; Prank, A.; Friedrichs, H.; Heil, R. D.; Herzberg, R. D.; Hoyler, F.; Van Isacker, P.; Kneissl, U.; et al. *Phys. Rev. Lett.* **1993**, *7*, 975-978.
- [5] Thouless, D. J. *Nucl. Phys.* **1961**, *22*, 78-95.
- [6] Pyatov, N. I.; Chernej, M. I. *Sov. J. Nucl. Phys.* **1972**, *16*, 931-940.
- [7] Kuliev, A. A.; Akkaya, R.; Ilhan, M.; Guliyev, E.; Salamov, C.; Selvi, S. *Int. J. Mod. Phys. E* **2000**, *9*, 249-261.
- [8] Goldstone, J.; Salam, A.; Weinberg, S. *Phys. Rev.* **1962**, *127*, 965-970.
- [9] Tabar, E.; Yakut, H.; Kuliev, A. A. *Int. J. Mod. Phys. E* **2016**, *25*, 1650053-1-1650053-24.
- [10] Tabar, E.; Yakut, H.; Kuliev, A. A. *Nucl. Phys. A* **2017**, *957*, 33-50.
- [11] Guliyev, E.; Kuliev, A. A.; Ertugral, F. *Nucl. Phys. A* **2013**, *915*, 78-89.
- [12] Zenginerler, Z.; Guliyev, E.; Kuliev, A. A.; Yakut, H.; Soluk, G. *Eur. Phys. J. A* **2013**, *49*, 1-7.

- [13] Kuliev, A. A.; Guliyev, E.; Ertugral, F.; Ozkan, S. *Eur. Phys. J. A* **2010**, *43*, 313-321.
- [14] Ziegler, W.; Rangacharyulu, C.; Richter, A.; Spieler, C. *Phys. Rev. Lett.* **1990**, *65*, 2515-2518.
- [15] Dudek, J.; Verner, T.; *J. Phys. G: Nucl. Part. Phys.* **1978**, *4*, 1543-1561.
- [16] Raman, S.; Nestor, C. W. Jr; Tikkanen, P. *At. Data Nucl. Data Tables* **2001**, *78*, 1-128.
- [17] Nosek, D.; Sheline, R. K.; Sood, P. C.; Kvasil J. Z. *Phys. A* **1993**, *344*, 277-283.
- [18] Lo Iudice, N.; Raduta, A. A. *Phys. Rev. C* **1993**, *50*, 127-137.
- [19] Garrido, E.; Guerra de Moya, E.; Sarriguren, P.; Udias, J. M. *Phys. Rev. C* **1991**, *44*, R1250-R1253.
- [20] Nord, J.; Enders, A. E.; De Almeida, P.; Belic, D.; Von Brentano, P.; Fransen, C.; Kneissl, U.; Kohstall, C.; Linnemann, A.; Von Neumann-Cosel, P.; et al. *Phys. Rev. C* **2003**, *67*, 034307-1-034307-23.
- [21] Enders, J.; Huxel, N.; Von Neumann-Cosel, P.; Richter, A. *Phys. Rev. Lett.* **1997**, *79*, 2010-2013.
- [22] Enders, J.; Huxel, N.; Kneissl, U.; Von Neumann-Cosel, P.; Pitz, H. H.; Richter, A. *Phys. Rev. C* **1998**, *57*, 996-999.